Distinct Targeting and Recycling Properties of Two Isoforms of the Iron Transporter DMT1 (NRAMP2, Slc11A2)†

Steven Lam-Yuk-Tseung and Philippe Gros*

Department of Biochemistry, McGill Cancer Center and Center for Host Resistance, McGill University, Montreal, Quebec H3G 1Y6, Canada

Received November 10, 2005; Revised Manuscript Received December 23, 2005

ABSTRACT: The metal transporter DMT1 (Slc11a2) plays a vital role in iron metabolism. Alternative splicing of the 3′ exon generates two DMT1 isoforms with different *C*-terminal protein sequences and a 3′ untranslated region harboring (isoform I, +IRE) or not (isoform II, −IRE), an iron-responsive element. Isoform I is expressed at the plasma membrane of certain epithelial cells including the duodenum brush border, where it is essential for the absorption of nutritional iron. Isoform II is expressed in many cells and is essential for the acquisiton of transferrin iron from acidified endosomes. The targeting and trafficking properties of DMT1 isoforms I and II were studied in transfected LLC-PK_1 kidney cells, with respect to isoform-specific differences in function, subcellular localization, endocytosis kinetics, and fate upon internalization. Isoform I showed higher surface expression and was internalized from the plasma membrane with slower kinetics than that of isoform II. As opposed to isoform II, which is efficiently sorted to recycling endosomes upon internalization, isoform I was not efficiently recycled and was targeted to lysosomes. Thus, alternative splicing of DMT1 critically regulates the subcellular localization and site of Fe^{2+} transport.

Our knowledge and understanding of iron metabolism has increased remarkably in recent years. Much of this knowledge stems from the discovery of proteins that play key roles in iron absorption and regulation, including the identification of membrane iron transporters (*1*). One such transporter, the divalent metal transporter 1 (DMT1,[11] also called Nramp2 or Slc11a2), is essential for intestinal iron acquisition and for iron uptake by peripheral tissues. DMT1 is an integral membrane phosphoglycoprotein consisting of 12 predicted trans-membrane segments (TM). DMT1 is part of a large, highly conserved family of metal transporters and has been shown to transport a number of divalent metals (Fe^{2+}, Mn^{2+}, Co^{2+}, Cu^{2+}, Cd^{2+}, Ni^{2+}, Pb^{2+}, and Zn^{2+}) in a pH-dependent fashion by a proton co-transport mechanism (*2*−*4*).

Genetic studies have shown that DMT1 plays a key role in iron metabolism. A G185R mutation in DMT1 causes microcytic anemia and iron deficiency in the *mk* mouse and in the *Belgrade* rat, two rodent models of iron deficiency (*5*−*10*). These animals show impaired iron uptake at the duodenal brush border and are also defective in iron acquisition in peripheral tissues including erythroid precursors (*10*−*13*). The G185R mutation likely causes misfolding of the protein, resulting in an altered subcellular localization (*9*, *14*−*16*), improper maturation, increased rate of degradation (*9*), and impaired transport activity. Recently, a human patient suffering from severe congenital hypochromic microcytic anemia and iron overload was shown to be homozygous for a mutation in DMT1 ($DMT1^{G1285C}$) (*17*, *18*). The human mutation had two effects. It severely impaired proper splicing of DMT1 mRNA and introduced an amino acid polymorphism (E399D) in the remaining properly spliced transcript found in the patient. The E399D mutation does not, in itself, affect expression, function, or targeting of the DMT1 protein (*19*, *20*), and thus the reduced DMT1 function in this patient is caused by reduced levels of DMT1 expression (improper splicing).

Two major DMT1 protein isoforms generated by alternative splicing at 3′ exons have been identified (*21*). Isoform I (+IRE) has an iron responsive element (IRE) in the 3′ untranslated region, whereas isoform II (−IRE) lacks the IRE. In addition, the *C*-terminal 18 amino acids of isoform I are replaced by an alternate 25 amino acid segment in isoform II. DMT1 isoform I is predominantly expressed in epithelial cells, whereas isoform II is predominantly expressed in erythroid cells. Indeed, the isoform I protein is expressed in enterocytes at the duodenal brush border (*22*) and epithelial cells lining the kidney proximal tubule (*16*), whereas isoform II is expressed abundantly in reticulocytes (*15*). However, preferential expression of each isoform is not necessarily mutually exclusive. The simultaneous expression of both DMT1 isoforms I and II mRNAs has been observed in several tissues, including the kidney, thymus, and liver (*2*, *23*, *24*). Recently, additional isoforms of DMT1 mRNAs have been identified on the basis of alternate

† This work was supported by a research grant from NIH (RO1 AI35237-10) to P.G. S.L. is supported by a doctoral studentship from the CIHR.

* To whom correspondence should be addressed. E-mail: philippe.gros@mcgill.ca. Tel: (514) 398-7291. Fax: (514) 398−2603.

[1] Abbreviations: DMT1, divalent metal transporter 1; Nramp2, natural resistance-associated macrophage protein 2; TM, transmembrane domain ; IRE, iron-responsive element; Lamp, lysosomal-associated membrane protein; HA, hemaglutinin; OPD, *o*-phenylenediamine dihydrochloride; HRP, horseradish peroxidase; GFP, green fluorescent protein; MESNA, 2-mercaptoethane sulfonate; EEA1, early endosome antigen 1.

10.1021/bi052307m CCC: $33.50
Published on Web 01/31/2006

promoter usage at DMT1 exon 1 (exon 1A vs 1B) (*25*). This alternate promoter would produce a predicted DMT1 protein with an additional 29 amino acids (exon 1A) located upstream from the previously identified start codon of DMT1 isoforms I and II (exon 1B). However, the role of these additional residues in the expression, function, and targeting of DMT1 has not yet been explored.

Although both DMT1 isoforms are expressed at the plasma membrane, isoforms I and II appear to show different subcellular targeting at a steady state. Although in transfected LLC-PK1, CHO, and RAW cells, DMT1 isoform II is expressed in early and recycling endosomes (*26*, *27*), studies in transfected HEp-2 cells indicate that isoform I is present in late endosomes and lysosomes (*23*). Recent studies using an exofacially tagged DMT1 molecule have furthered our understanding of isoform II trafficking: Isoform II molecules present at the cell surface and in recycling endosomes are in dynamic equilibrium, with surface transporters being continuously internalized via a clathrin- and dynamin-dependent process (*27*). Tabuchi and colleagues have shown that a $YXLXX^{555-559}$ motif in the *C* terminus of DMT1 isoform II is responsible for the early endosome targeting of the protein, with mutations in this motif resulting in lysosomal localization (*23*). Recently, we have shown that critical residues in the *C* terminus of DMT1 isoform II, including the $YXLXX^{555-559}$ signal, are required for the transporter's internalization from the cell surface and its recycling back to the plasma membrane (*28*). Removal of an intact $YXLXX^{555-559}$ motif appears to cause lysosomal targeting by default.

Although DMT1 isoform II trafficking has been well studied, much less is known about the subcellular distribution, targeting, and dynamic trafficking of the DMT1 intestinal isoform I. Whereas isoform I lacks the YXLXX signal present in isoform II, close examination of the *C* terminus of isoform I reveals the presence of a dileucine motif ($LL^{550,551}$). Dileucine-based (LL) motifs present in a number of membrane proteins have been alternately shown to act as signals for clathrin-mediated endocytosis or for targeting various endosomes/lysosomes (*29*). In this study, we wanted to investigate possible trafficking differences between isoform I and II of DMT1. We expressed exofacially tagged DMT1-HA proteins in a porcine kidney epithelial cell line and studied the differences between expression, function, subcellular localization, internalization kinetics, and fate upon the internalization of DMT1 isoforms I and II. We found that DMT1 isoform I is internalized with slower kinetics from the cell surface compared to that of isoform II. This results in an increased proportion of isoform I expressed at the plasma membrane, perhaps favoring iron transport at this site in epithelial cells.

MATERIALS AND METHODS

Materials and Plasmids. All reagent-grade chemicals were purchased from Sigma Chemical (St. Louis, MO). Monoclonal mouse antibody (Ab) HA.11 directed against the influenza hemagglutinin epitope (HA) was purchased from Covance (Princeton, NJ). Cy3-labeled anti-rabbit and anti-mouse Ab's and HRP-coupled donkey antimouse Ab were purchased from Jackson Immuno Research Laboratories (West Grove, PA). Plasmids encoding GFP-fusion proteins were kind gifts from Dr. D. Williams (Department of Biochemistry, University of Toronto; GFP-syntaxin 13) and Dr. Patrice Boquet (Institut national de la santé et de la recherché médicale, France; GFP-Lamp1). Full-length murine DMT1 isoform I (+IRE, isoform 1A) and isoform II (−IRE, isoform 1B) cDNAs were modified by the in-frame addition of an HA epitope in the fourth extracellular loop, as previously described (*4*).

Cell Culture, Transfection, and Immunoblotting. LLC-PK_1 cells were cultured in a 37 °C, 5% CO_2 incubator in Dulbecco's modified Eagle's medium (Invitrogen) supplemented with 10% fetal bovine serum (growth media). Cells were transfected with DMT1-HA/pCB6 vectors using Lipofectamine2000 (Invitrogen), according to the manufacturer's instructions. Selection of stably transfected clones was done using 1.4 mg/mL of G418 (Invitrogen) for 14 days. Individual colonies were then isolated and expanded. Total cell lysates were prepared and separated by SDS−PAGE. Clones showing robust DMT1-HA expression were identified by immunoblotting with mouse anti-HA antibody, as previously described (*30*).

Calcein Divalent Metal Transport Assay. Calcein acetoxymethylester (calcein-AM, molecular probes) was prepared in dimethyl sulfoxide. Fe^{2+} and Co^{2+} solutions were freshly prepared in deionized water as 2 mM stock solutions of ferrous ammonium sulfate and cobalt chloride, respectively. Measurement of metal transport in DMT1-HA-transfected LLC-PK1 cells was done using a fluorescence quenching assay, as previously described (*20*). Initial rates of metal transport (quench rates) were calculated from fluorescence quenching curves.

Immunostaining. Cells were fixed with 4% paraformaldehyde/PBS for 20 min and where indicated were blocked and permeabilized with 0.2% saponin/5% nonfat milk/PBS for 30 min. For co-localization with EEA1 (Figure 5A), cells were blocked in 5% nonfat milk (for 30 min) and permeabilized with 0.1% Triton X-100/PBS (for 30 min), following fixation. All antibody incubations were performed for 1 h at room temperature and diluted in blocking solution, unless otherwise indicated. Primary Ab's were used at the following dilutions: rabbit anti-DMT1, 1:200; mouse anti-HA 1:100; and goat anti-EEA1, 1:200; corresponding secondary Ab's (goat anti-rabbit Cy3, goat anti-mouse Cy3, and donkey anti-goat Alexa 488, respectively) were each used at 1:1000. For co-localization with GFP-fusion proteins (Figures 2 and 5B), cells were transfected with GFP-syntaxin 13 or GFP-Lamp1 plasmids, 24 h prior to fixation using Lipofectamine2000. For labeling of cell surface DMT1-HA molecules (Figure 3A), cells were fixed, blocked in 5% nonfat milk for 30 min, and labeled with anti-HA primary Ab and the secondary Ab without permeabilizing the cells with detergent. For experiments with live cells (Figure 5), anti-HA antibody was diluted (1:200) in RPMI medium, and (where indicated) the cells were chased by washing twice and then incubating the cells in growth media for 90 min at 37 °C. Cells were visualized using an Axiovert 200M epifluorescence microscope with a 100× oil immersion objective. Digital images were acquired with a Zeiss AxioCam HRm camera operated with AxioVision 4.3. Images were cropped, assembled, and labeled using Adobe Photoshop and Illustrator softwares.

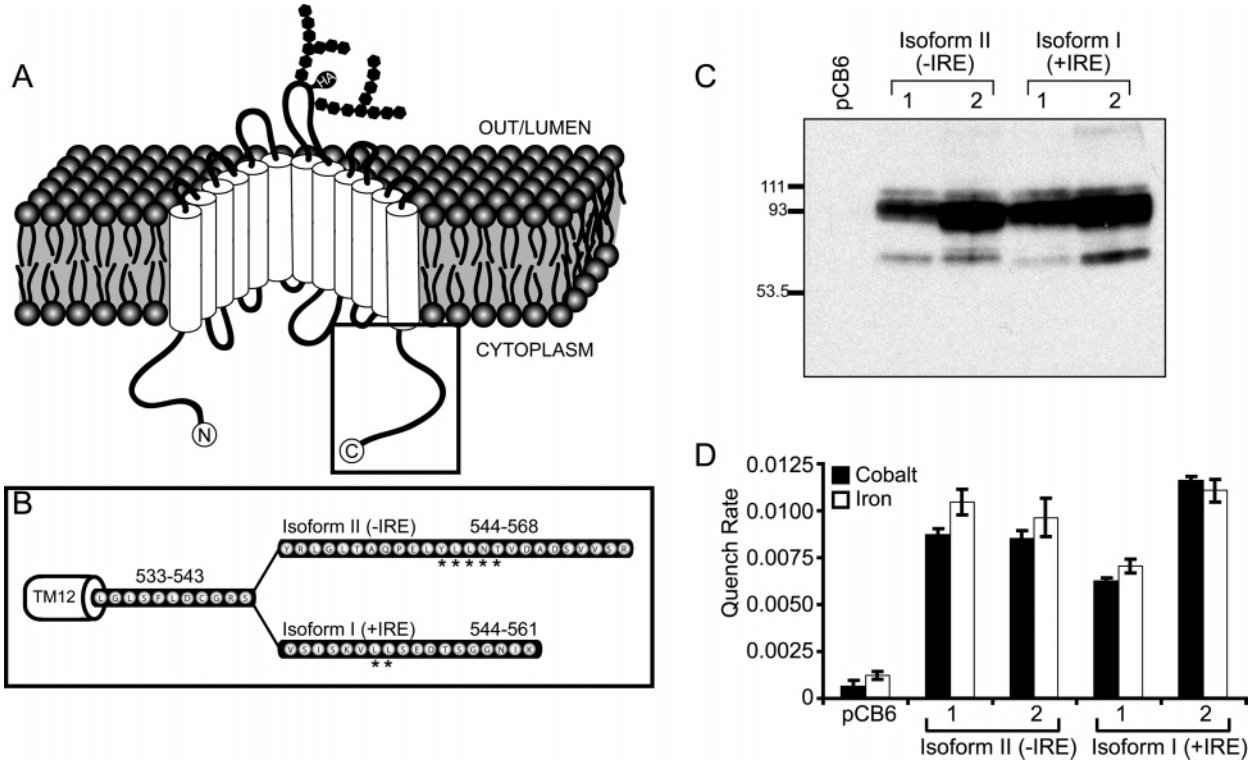

FIGURE 1: Expression and functional activity of DMT1 isoforms I and II in LLC-PK_1 cells. (A) A schematic representation of the DMT1-HA protein, highlighting the positions of the inserted exofacial hemagglutinin (HA) epitope, predicted asparagine-linked glycosylation sites (hexagons), and the carboxyl terminus (boxed). (B) A comparison of the *C*-terminal sequences of DMT1 isoforms I and II. Predicted sorting/trafficking signal sequences are highlighted (*). We prepared extracts from LLC-PK_1 cells transfected with the vector (pCB6) or independent clones (1 and 2) stably expressing DMT1 isoforms I and II. Equal amounts of each extract was resolved by SDS−PAGE. (C) A representative immunoblot performed with an anti-HA Ab. The sizes of molecular weight standards (in kilodaltons) are indicated. (D) Metal transport activity of cells stably transfected with vector only (pCB6) or DMT1 isoforms I and II. Cells loaded with a metal-sensitive fluorescent dye were incubated with Fe^{2+} or Co^{2+} in an acidic buffer. The results are shown as the initial rates of fluorescence quenching. Error bars represent standard error of the means of three or more independent determinations.

Measurement of Surface DMT1-HA at Steady State. Quantification of the proportion of DMT1-HA molecules expressed at the cell surface has been previously described (*20*). Briefly, LLC-PK_1 cells were grown to confluency in 48-well culture plates and fixed with 4% paraformaldehyde for 30 min. Cells were blocked in 5% nonfat milk in PBS for 30 min, incubated with anti-HA Ab (1:500) for 90 min, washed, and incubated with secondary Ab (donkey anti-mouse-HRP Ab, 1:4000) for 1 h. For the quantification of total DMT1-HA expression, the cells were permeabilized by incubation with 0.1% Triton X-100/PBS for 30 min prior to incubation with anti-HA Ab. Peroxidase activity was detected by incubating cells with the HRP substrate (0.4 mg/mL *o*-phenylenediamine dihydrochloride, Sigma FAST OPD) according to the manufacturer's instructions. Reactions were stopped after 30 min with 3 M HCl, and absorbance readings (492 nm) were taken with a spectrometer. For all assays, background absorbance readings from (a) the nonspecific binding of the secondary Ab and (b) the nonspecific binding of the primary Ab to vector-transfected cells were subtracted for each sample. Cell surface readings were normalized to total DMT1-HA values for each cell clone and were expressed as a percentage.

Cell Surface Biotinylation. The measurement of DMT1 internalization by cell surface biotinylation has been previously described (*28*). Briefly, confluent LLC-PK1 monolayers were biotinylated at 4 °C in a borate buffer at pH 9.0, containing 1 mg/mL sulfo-NHS-SS-biotin (Pierce). Cells were washed and incubated in prewarmed RPMI for 0, 30, 60, or 90 min at 37 °C, at which point endocytosis was halted by washes with cold PBS. Cell-surface-associated biotin molecules were removed by three cold washes with the membrane-impermeable reducing agent 2-mercaptoethanesulfonic acid (MESNA, 100 mM solution). For the quantification of total surface labeling, cells were similarly treated but with final washes in a buffer lacking MESNA. Biotinylated cells were collected and solubilized in a lysis buffer with protease inhibitors. Lysates were precleared by centrifugation, and the protein yield was quantified. Biotinylated proteins (200 μg total protein lysate) were isolated by overnight incubation at 4 °C with 100 μL of ImmunoPure immobilized strepavidin slurry (Pierce) in a final volume of 1 mL in a lysis buffer. Strepavidin beads were washed four times with a cold lysis buffer, and bound proteins were eluted with 2× Laemmli buffer at room temperature for 30 min. Proteins were separated by SDS−PAGE, followed by immunoblotting with anti-HA Ab. The intensity of the immunoreactive bands were quantified by a densitometry analysis of the exposed films using a Fuji LAS-1000. Background intensity readings (after 0 min of endocytosis) were subtracted from all readings, and the results were expressed as a percentage of total surface labeling for each clone.

RESULTS

Expression and Functions of DMT1 Isoforms I and II. To investigate the subcellular localization and trafficking proper-

ties of the two DMT1 protein isoforms, we modified the mouse DMT1 isoforms I and II cDNAs by inserting an exofacial hemagglutinin (HA) tag into the extracellular loop of the protein defined by the predicted TM7 and 8 (Figure 1A). This exofacial tag enabled us to label and track cell-surface expressed DMT1-HA molecules in intact cells. We have previously shown that the insertion of an HA tag at this position does not affect the expression, transport activity, or subcellular localization of DMT1 (*27*). We generated stably transfected cells expressing DMT1 isoforms I and II in the porcine LLC-PK_1 kidney cell line. LLC-PK_1 cells were chosen because they are derived from the kidney proximal tubule, an abundant site of DMT1 protein expression in normal tissues (*16*). Therefore, these cells are likely to express the necessary cellular machinery for proper DMT1 trafficking, including the recognition of sorting and targeting signals. Figure 1C illustrates a representative immunoblot of cell extracts prepared from two independent LLC-PK_1 cell clones expressing different levels of DMT1 isoforms I or II. In each case, a minor species at ~60 kDa and a major species at ~90 kDa were observed. Previous studies from our group have shown that these two populations correspond to core and complex glycosylated species of DMT1, respectively (*27*). These observations show that both isoforms of DMT1 are stably expressed and glycosylated to a similar extent in LLC-PK_1 cells. Experiments with the protein translation inhibitor cycloheximide revealed that DMT1 isoforms I and II show similar stability in LLC-PK_1 cells (Supporting Information). Finally, we tested the ability of DMT1 isoforms I and II to transport divalent metals (Fe^{2+} and Co^{2+}) at acidic pH by calcein fluorescence quenching. Independent clones from both DMT1 isoforms I and II showed robust transport activity compared to that of vector-transfected cells (pCB6). No difference in transport rates or ion selectivity between the two isoforms was detected, indicating that both isoforms are expressed at the cell surface and properly folded in a transport-competent manner (Figure 1D).

Subcellular Localization of DMT1 Isoforms I and II. The subcellular localization of DMT1 isoforms I and II was determined by double immunofluorescence with an anti-DMT1 antibody, using fixed and permeabilized cells. As reported earlier, DMT1 isoform II was detected in an endomembrane compartment, where it displayed strong co-localization with the recycling endosome marker, GFP-syntaxin 13 (Figure 2A), but showed little overlap with the late endosome and lysosomal marker, GFP-Lamp1 (Figure 2B) (*27*, *28*). Conversely, DMT1 isoform I was detected in endomembrane vesicles of a larger size than those positive for isoform II, which showed little co-localization with GFP-syntaxin 13 (Figure 2A) but strong co-localization with GFP-Lamp1 (Figure 2B). These results indicate that the two DMT1 isoforms are differentially targeted at steady state in LLC-PK_1 cells: isoform II to recycling endosomes and isoform I to late endosomes and lysosomes.

Our transport data in intact cells (Figure 1D) also suggested that both isoforms were present in a functional state at the cell surface. Therefore, we used immunofluorescence microscopy to investigate the cell surface expression of each isoform. Surface-expressed DMT1-HA molecules were visualized by incubating fixed but unpermeabilized LLC-PK_1 transfected cells with anti-HA antibody followed by labeling with a conjugated-fluorescent secondary

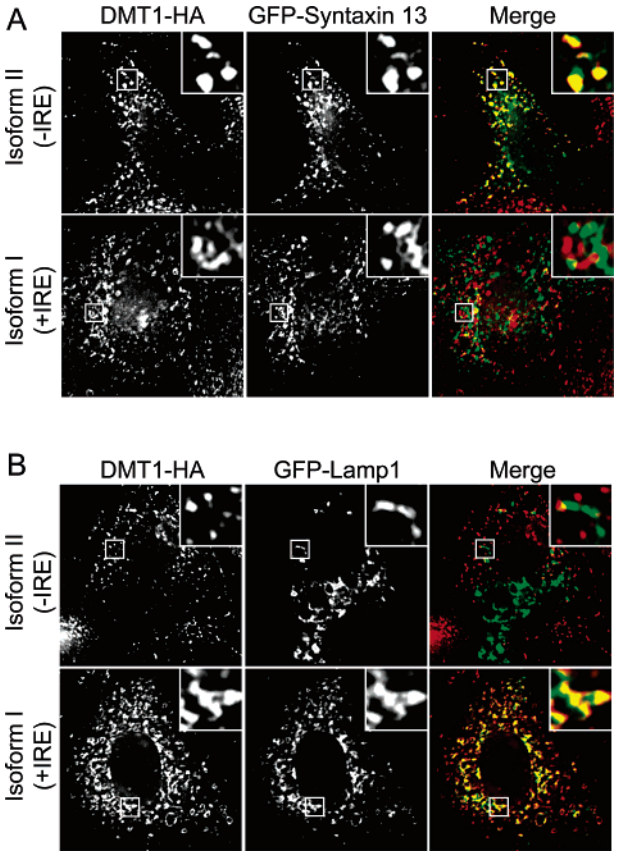

FIGURE 2: Subcellular localization of DMT1 isoforms I and II in LLC-PK_1 cells. LLC-PK_1 cells stably expressing DMT1 isoforms I and II were transiently transfected with either (A) GFP-syntaxin 13 to label recycling endosomes or (B) GFP-Lamp1 to label late endosomes and lysosomes. After 24 h, the cells were fixed, permeabilized, and stained with an anti-DMT1 antibody. DMT1 molecules were visualized using a secondary antibody coupled to fluorescent Cy3. The images were acquired by epifluorescence microscopy. The insets show the magnifications of the area that is boxed.

antibody. Interestingly, isoform I displayed a much stronger surface expression compared to that of isoform II (Figure 3A). We quantified this difference in surface expression using a horseradish peroxidase-conjugated secondary antibody and found that a significantly higher proportion of total DMT1 isoform I (clone 1, 44.5 ± 2.8%; clone 2, 45.6 ± 1.5%; mean ± SE) was expressed at the plasma membrane compared to that of isoform II (clone 1, 24.8 ± 2.0%; clone 2, 24.4 ± 1.6%) (Figure 3B). Thus, despite similar levels of total DMT1 protein expression in the pair of LLC-PK_1 clones tested, isoform I shows a higher cell surface expression than isoform II.

Endocytosis. The different levels of cell surface expression and apparent variations in intracellular localization of isoforms I and II suggested that the two proteins had different trafficking properties. Therefore, we measured the rates of endocytosis from the plasma membrane of isoforms I and II using a cell surface biotinylation technique (*28*). We used a membrane impermeable, cleavable biotin compound to covalently label all surface-exposed plasma membrane proteins in LLC-PK_1 cells that were cooled to 4 °C to halt endocytosis. Following biotinylation, the cells were warmed to 37 °C for 0 to 90 min to allow the internalization of labeled plasma membrane proteins. Biotin molecules remaining at the cell surface were removed by washing the cells with a

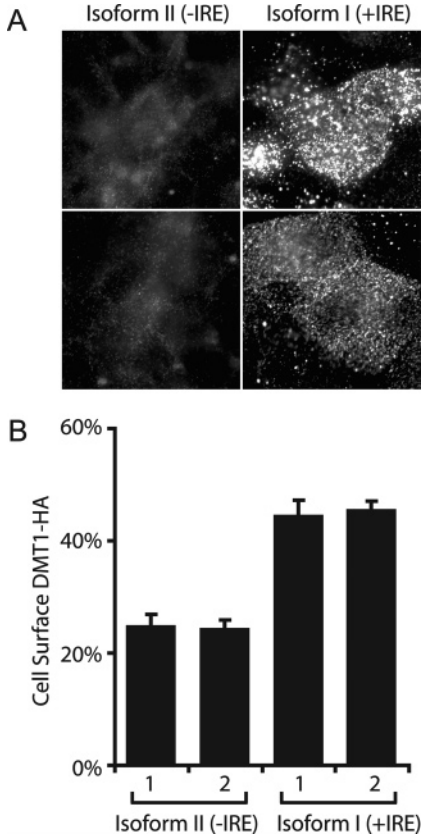

FIGURE 3: Quantification of cell surface expression of DMT1 isoforms I and II in LLC-PK$_1$ cells. LLC-PK$_1$ cells stably expressing DMT1 isoforms I and II were fixed, and surface DMT1 molecules were labeled by incubating the cells with a primary anti-HA antibody without permeabilization, followed by a secondary antibody coupled to Cy3 (A) The images were acquired by epifluorescence microscopy. (B) A quantification of the fraction of DMT1-HA molecules expressed at the cell surface. Cells were fixed and incubated with primary anti-HA antibody with or without prior detergent permeabilization (Materials and Methods). Cells were then incubated with an HRP-coupled secondary antibody, and the amount of bound primary antibody present was determined for both conditions by a colorimetric reaction using *o*-phenylenediamine dihydrochloride (OPD) followed by spectrometry. The amount of DMT1-HA expressed at the cell surface (in nonpermeabilized cells) is shown as a fraction (%) of total protein expression (in permeabilized cells).

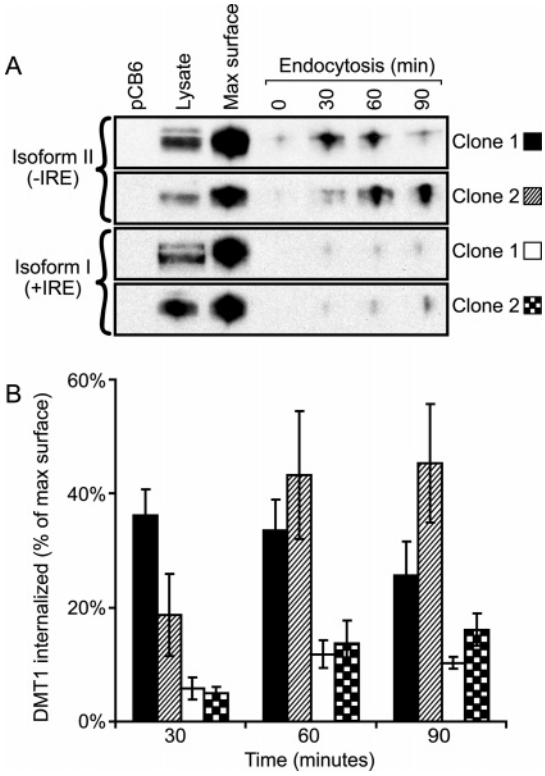

FIGURE 4: Quantification of the rate of endocytosis of DMT1 isoforms I and II in LLC-PK$_1$ cells. A cell surface biotinylation assay was used to compare internalization rates of DMT1 isoforms I and II from the plasma membrane. We used a membrane impermeable, cleavable biotin reagent to label surface proteins. The labeling was performed at 4°C to halt endocytosis. Internalization of surface proteins was allowed to occur at 37 °C for 0−90 min. After that time, biotin molecules remaining at the surface were removed, and biotinylated proteins were isolated from cell lysates with immobilized strepavidin. Proteins were resolved by SDS−PAGE, and DMT1 molecules were detected by immunoblotting with anti-HA antibody. (A) Typical immunoblots from individual experiments done on independent clones (1 and 2). Immunoblots were scanned by densitometry, and (B) the amount of DMT1 internalized over time is expressed as a fraction (%) of the total cell surface expression (max). Lysate = 20 μg of unbiotinylated crude cell lysate for each mutant; max = total surface DMT1-HA expression for each clone (biotinylated DMT1-HA molecules isolated without prior stripping). Error bars correspond to standard errors of the means from three or more independent experiments.

membrane-impermeable reducing agent. Cells were solubilized, and biotinylated DMT1-HA molecules were isolated using immobilized streptavidin, followed by SDS−PAGE and immunoblotting with anti-HA antibody. Figure 4A illustrates a typical immunoblot, and the quantification of three different immunoblots by densitometric scanning is shown in Figure 4B. Intracellular accumulation of surface-labeled DMT1-HA molecules after 0 to 90 min was expressed as a percentage of the maximal surface DMT1-HA (without washing with a reducing agent) after 0 min (Figure 4B). Strikingly, independent clones of DMT1 isoform II displayed a significantly higher internalization at each time point compared to that of independent clones of DMT1 isoform I. The greatest difference occurred after 60 min with isoform II clones showing 33.6 ± 5.4 and 43.2 ± 11.2% of cell surface DMT1-HA internalized compared to 11.8 ± 2.4 and 13.8 ± 3.9% for isoform I clones. These results demonstrate that the higher plasma membrane expression of isoform I is correlated with a reduced rate of internalization from the cell surface compared to that of isoform II. Indirectly, these results suggest that the carboxyl terminal cytoplasmic tail of isoform I lacks the endocytosis signal present in the carboxyl tail of isoform II.

Fate of Internalized DMT1 Molecules. Having shown that DMT1 isoform I is internalized with slower kinetics from the cell surface, we next investigated the fate of internalized isoform I molecules. We labeled surface/internalized DMT1-HA molecules in live LLC-PK$_1$ cells by incubating the cells with anti-HA antibody at 37 °C in a culture medium for 2 h. The cells were fixed, permeabilized, and labeled with an antibody against EEA1, a marker of early endosomes. Both isoforms of DMT1 showed significant co-localization with EEA1 (blue arrowheads in Figure 5A). To determine the fate of internalized DMT1 molecules after a longer incubation period, the cells were labeled for 3 h, washed, and chased in culture media for an additional 90 min. Lysosomes were labeled by transient transfection with GFP-Lamp1, 24 h prior to labeling. As expected, isoform II did not show significant

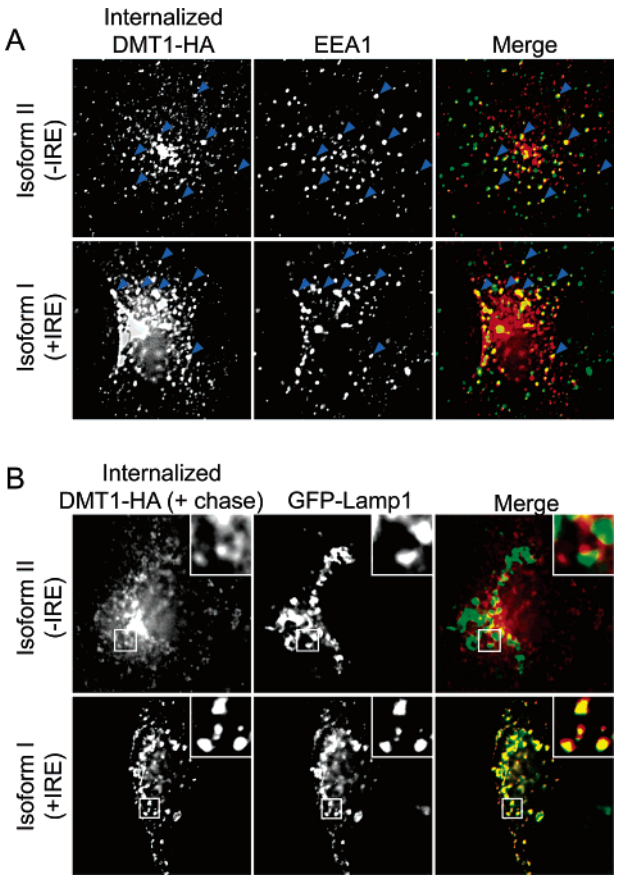

FIGURE 5: Fate of internalized DMT1 isoform I and II molecules. (A) LLC-PK$_1$ cells expressing either DMT1 isoform I or isoform II were incubated with anti-HA antibody for 2 h to label cell surface and recycling DMT1-HA molecules. To investigate co-localization of internalized DMT1-HA molecules with early endosomes, cells were fixed, permeabilized, and incubated with an antibody against the early endosomal marker EEA1. DMT1 molecules were visualized using a fluorescent secondary antibody. Areas showing overlapping staining are highlighted (blue arrowheads). (B) To investigate co-localization of DMT1 isoforms with lysosomes, cells were transiently transfected with the lysosomal marker GFP-Lamp1. After 24 h, surface and recycling DMT1-HA molecules were labeled with anti-HA Ab for 3 h, washed, and chased by incubation in growth media for 90 min. Cells were fixed, permeabilized, and stained with an anti-mouse fluorescent secondary Ab to visualize DMT1-HA molecules. The insets show the magnifications of the area that is boxed. The images were acquired by epifluorescence microscopy.

co-localization with Lamp1 (Figure 5B), indicating that the protein was efficiently recycled back to the cell surface. Strikingly, in cells labeled for 3 h, isoform I showed a strong co-localization with the lysosomal marker (Figure 5B). These results show that DMT1 isoform I, upon internalization and passage through early endosomes, fails to recycle back to the plasma membrane and is targeted to late endosomes and lysosomes. These results suggest that the carboxyl terminus of isoform I not only lacks an endocytosis signal but also a recycling signal present in the carboxyl terminus of isoform II. Slower endocytosis of isoform I from the plasma membrane results in elevated cell surface expression at steady state (Figure 3).

DISCUSSION

DMT1 isoform II is expressed in many cell types but is particularly abundant in erythroid precursors (*15*). Studies in transfected cells in vitro have shown that isoform II is rapidly internalized along with the transferrin receptor from the plasma membrane by a clathrin- and dynamin-dependent process (*27*). Endosomal acidification facilitates the release of iron from transferrin and provides the proton gradient for DMT1-mediated iron transport across the endosomal membrane. Iron is then stored, bound to ferritin, or transported into mitochondria for heme synthesis. DMT1 isoform II and the transferrin receptor are subsequently recycled back to the cell surface. The critical role of DMT1 in this iron-acquisition process is highlighted by the recent report that a patient with a mutation in DMT1 suffers from erythroid hyperplasia with defective hemoglobinization (*17*). In circulation, a majority of iron is bound to transferrin and very little iron exists in its free cationic form. This correlates well our data as well as earlier reports that less than 35% of total DMT1 isoform II is expressed at the cell surface, with a majority of isoform II residing in transferrin receptor-positive recycling endosomes.

Directional or trans-cellular transport is essential in epithelial cells located at the sites of absorption or reabsorption of key elements such as iron. Dietary nonheme iron is mainly absorbed at the duodenal brush border. DMT1, expressed at the apical pole of enterocytes lining the intestinal lumen, transports iron across the apical membrane, whereas ferroportin, expressed at the basal pole, transports iron across the basolateral membrane. It is predominantly the isoform I variant of DMT1 that is expressed at the apical membrane of enterocytes (*22*). Our finding that cell surface expression of isoform I in LLC-PK$_1$ cells is higher than that of isoform II is in agreement with the noted preferential expression of isoform I at the cell surface of different cell types in vivo (compared to that of isoform II), namely the brush border of epithelial cells of the duodenum and the kidney proximal tubule. We also found that isoform I is not efficiently recycled upon internalization and is ultimately targeted to lysosomes. These findings indicate that iron transported by isoform I (at the duodenal brush border) involves the direct transfer of Fe^{2+} from the intestinal lumen into the cytoplasm of enterocytes, in the absence of an active Tf−TfR cycle at the apical poles of these cells. However, TfR is expressed at the basolateral membrane and in the basal recycling endosomes of intestinal epithelial cells (*31*, *32*), and it is possible that DMT1 isoform II may play an additional role in iron acquisition at that site as well (*23*). In addition, mutagenesis studies suggested that N-linked glyosylation of DMT1 controls apical versus basolateral targeting in polarized cells (*23*). Thus, it is possible that the trafficking differences between DMT1 isoforms I and II in epithelial cells may not only involve the differential targeting to the plasma membrane but also be influenced by the different rates of internalization of the transporters from the cell surface, as demonstrated here in transfected LLC-PK$_1$ cells. In addition, recent work by Johnson and colleagues in Caco-2 cells suggests that isoform I trafficking may be regulated by cellular iron levels. This result emphasizes the importance of isoform-specific trafficking in overall DMT1 function, including coupling to the Tf−TfR cycle (*24*).

Although targeting and dynamic sorting/recycling of DMT1 isoform II has been thoroughly studied by us and others, much less is known about isoform I. The protein sequences of isoforms I and II differ only in their *C*-terminal

segments (Figure 1B). In isoform II, Tabuchi and colleagues have shown that a YLLNT$^{555-559}$ signal in the *C* terminus of the protein is required for its early endosome targeting in HEp-2 larynx carcinoma cells (*23*). We have previously shown that the *C* terminus of isoform II, along with the YLLNT signal, is vital for the internalization of the protein from the cell surface and its recyclization back to the plasma membrane in LLC-PK$_1$ epithelial cells (*28*). Critical mutations or deletions at YLLNT result in severely impaired internalization, accumulation of the transporter at the cell surface, and failure of the protein to recycle properly, resulting in lysosomal targeting. DMT1 isoform I lacks an endogenous YLLNT motif in its carboxyl terminus. Interestingly, the trafficking properties of the isoform II YLLNT mutants (including a *C*-terminal truncation) virtually mirror the trafficking properties of DMT1 isoform I reported here (*28*). These findings together with the results of the present study demonstrate the critical role of the YLLNT sequence motif as a recycling motif in DMT1. Furthermore, these results argue against the presence of a functional targeting motif in the *C*-terminal region of DMT1 isoform I.

Examination of the *C*-terminal sequence of isoform I reveals the presence of a putative dileucine motif (LL$^{550-551}$, Figure 1B). Indeed, cytoplasmic dileucine-based (LL) motifs of membrane proteins often act as signals leading to clathrin-mediated endocytosis or targeting to endosomal−lysosomal compartments (*33*−*36*). Residues neighboring the LL signals appear to dictate whether clathrin recruitment occurs via AP complexes or via ARF-dependent clathrin adaptors (*29*). Dileucine-based signals usually fit either the [DE]XXXL-[LI] or DXXLL consensus motifs. [DE]XXXL[LI] signals are specifically recognized by AP complexes, and DXXLL signals are recognized by GGAs, a recently described family of ARF-dependent clathrin adaptors. However, the amino acids preceding the dileucine motif in DMT1 isoform I (SISKV$^{545-549}$) do not fit either of these consensus motifs. Therefore, the relevance of this leucine pair (LL^{550,551}) in the targeting and sorting of isoform II remains unclear and awaits further characterization.

On the basis of previous work and data reported here, we propose a model for the subcellular trafficking of the two isoforms of DMT1. In this model, DMT1 proteins would be synthesized in the endoplasmic reticulum, posttranslationally modified in the Golgi apparatus, and targeted to the plasma membrane. Isoform II molecules are then rapidly internalized from the cell surface by recruiting specific adaptor proteins required for clathrin-mediated endocytosis (*27*), which we propose interact with the YLLNT motif and possibly other determinants in the *C*-terminal region of the transporter. Isoform II is internalized into early endosomes, and the recruited adaptor complexes are involved in recycling the transporter back to the cell surface via targeting to recycling endosomes (Figure 6). This pathway ensures that the isoform II molecules expressed in erythroid cells work in conjunction with transferrin receptors in the uptake of transferrin-iron. DMT1 isoform I molecules lack the YLLNT motif and would be unable to recruit clathrin/adaptor complexes at the plasma membrane. Consequently, isoform I transporters are internalized into early endosomes by a kinetically slower mechanism such as bulk pinocytosis (Figure 6). The slower rate of endocytosis of isoform I results in a greater fraction of the DMT1 variant expressed at the cell surface at steady state.

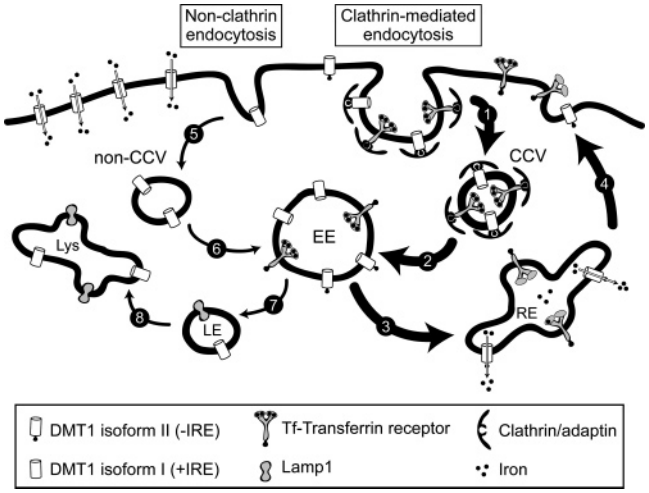

FIGURE 6: Schematic model for the distinct trafficking of DMT1 isoforms I and II. DMT1 molecules are synthesized in the endoplasmic reticulum, posttranslationally modified in the Golgi apparatus, and targeted to the plasma membrane by default. Clathrin molecules interact with surface DMT1 isoform II (−IRE) molecules via adaptins that specifically recognize the tyrosine-based motif YLLNT and possibly other residues present in the *C* terminus of the variant. Isoform II molecules are rapidly internalized (step 1) by a dynamin-dependent process into clathrin-coated vesicles (CCV). DMT1-containing CCVs are sorted first to early endosomes (EE, step 2), followed by recycling endosomes (RE, step 3). The acidic environment of RE favors the release of iron from transferrin and creates the proton gradient required for iron transport by DMT1 isoform II. In contrast, surface DMT1 isoform I molecules, which lack the *C*-terminal tyrosine-based sorting motif, are internalized less rapidly by a clathrin-independent mechanism into nonCCVs (step 5). Isoform I molecules are sorted to EE (step 6) but are not efficiently recycled back to the cell surface and are eventually targeted to Lamp1-positive late endosomes and lysosomes (steps 7 and 8).

However, failure of isoform I molecules to recruit specific recycling adaptor complexes prohibits their sorting to recycling endosomes and leads to an accumulation in the late endosomes and lysosomes. This trafficking pathway ensures a high level of DMT1 isoform I expression at the plasma membrane of epithelial cells, favoring the absorption/reabsorption of iron.

Overall, our findings highlight the critical role of alternate splicing at the 3′ end of the DMT1 gene for the generation of protein isoforms that transport iron at different subcellular sites in a transferrin-dependent (isoform II), and transferrin-independent (isoform I) manner.

ACKNOWLEDGMENT

P.G. is the recipient of a Distinguished Scientist award from the Canadian Institutes of Health Research (CIHR) and is a James McGill Professor of Biochemistry.

SUPPORTING INFORMATION AVAILABLE

Data from experiments with the protein translation inhibitor cycloheximide. This material is available free of charge via the Internet at http://pubs.acs.org.

REFERENCES

1. Hentze, M. W., Muckenthaler, M. U., and Andrews, N. C. (2004) Balancing acts: molecular control of mammalian iron metabolism, *Cell 117*, 285−297.

2. Gunshin, H., Mackenzie, B., Berger, U. V., Gunshin, Y., Romero, M. F., Boron, W. F., Nussberger, S., Gollan, J. L., and Hediger, M. A. (1997) Cloning and characterization of a mammalian proton-coupled metal-ion transporter, *Nature 388*, 482−488.
3. Forbes, J. R., and Gros, P. (2003) Iron, manganese, and cobalt transport by Nramp1 (Slc11a1) and Nramp2 (Slc11a2) expressed at the plasma membrane, *Blood 102*, 1884−1892.
4. Picard, V., Govoni, G., Jabado, N., and Gros, P. (2000) Nramp 2 (DCT1/DMT1) expressed at the plasma membrane transports iron and other divalent cations into a calcein-accessible cytoplasmic pool, *J. Biol. Chem. 275*, 35738−35745.
5. Fleming, M. D., Romano, M. A., Su, M. A., Garrick, L. M., Garrick, M. D., and Andrews, N. C. (1998) Nramp2 is mutated in the anemic Belgrade (b) rat: evidence of a role for Nramp2 in endosomal iron transport, *Proc. Natl. Acad. Sci. U.S.A. 95*, 1148−1153.
6. Fleming, M. D., Trenor, C. C., III, Su, M. A., Foernzler, D., Beier, D. R., Dietrich, W. F., and Andrews, N. C. (1997) Microcytic anaemia mice have a mutation in Nramp2, a candidate iron transporter gene, *Nat. Genet. 16*, 383−386.
7. Russell, E. S., Nash, D. J., Bernstein, S. E., Kent, E. L., McFarland, E. C., Matthews, S. M., and Norwood, M. S. (1970) Characterization and genetic studies of microcytic anemia in house mouse, *Blood 35*, 838−850.
8. Su, M. A., Trenor, C. C., Fleming, J. C., Fleming, M. D., and Andrews, N. C. (1998) The G185R mutation disrupts function of the iron transporter Nramp2, *Blood 92*, 2157−2163.
9. Touret, N., Martin-Orozco, N., Paroutis, P., Furuya, W., Lam-Yuk-Tseung, S., Forbes, J., Gros, P., and Grinstein, S. (2004) Molecular and cellular mechanisms underlying iron transport deficiency in microcytic anemia, *Blood 104*, 1526−1533.
10. Edwards, J. A., and Hoke, J. E. (1972) Defect of intestinal mucosal iron uptake in mice with hereditary microcytic anemia, *Proc. Soc. Exp. Biol. Med. 141*, 81−84.
11. Edwards, J. A., and Hoke, J. E. (1975) Red cell iron uptake in hereditary microcytic anemia, *Blood 46*, 381−388.
12. Edwards, J. A., Garrick, L. M., and Hoke, J. E. (1978) Defective iron uptake and globin synthesis by erythroid cells in the anemia of the Belgrade laboratory rat, *Blood 51*, 347−357.
13. Edwards, J. A., Sullivan, A. L., and Hoke, J. E. (1980) Defective delivery of iron to the developing red cell of the Belgrade laboratory rat, *Blood 55*, 645−648.
14. Canonne-Hergaux, F., Fleming, M. D., Levy, J. E., Gauthier, S., Ralph, T., Picard, V., Andrews, N. C., and Gros, P. (2000) The Nramp2/DMT1 iron transporter is induced in the duodenum of microcytic anemia mk mice but is not properly targeted to the intestinal brush border, *Blood 96*, 3964−3970.
15. Canonne-Hergaux, F., Zhang, A. S., Ponka, P., and Gros, P. (2001) Characterization of the iron transporter DMT1 (NRAMP2/DCT1) in red blood cells of normal and anemic mk/mk mice, *Blood 98*, 3823−3830.
16. Canonne-Hergaux, F., and Gros, P. (2002) Expression of the iron transporter DMT1 in kidney from normal and anemic mk mice, *Kidney Int. 62*, 147−156.
17. Mims, M. P., Guan, Y., Pospisilova, D., Priwitzerova, M., Indrak, K., Ponka, P., Divoky, V., and Prchal, J. T. (2005) Identification of a human mutation of DMT1 in a patient with microcytic anemia and iron overload, *Blood 105*, 1337−1342.
18. Priwitzerova, M., Pospisilova, D., Prchal, J. T., Indrak, K., Hlobilkova, A., Mihal, V., Ponka, P., and Divoky, V. (2004) Severe hypochromic microcytic anemia caused by a congenital defect of the iron transport pathway in erythroid cells, *Blood 103*, 3991−3992.
19. Priwitzerova, M., Nie, G., Sheftel, A. D., Pospisilova, D., Divoky, V., and Ponka, P. (2005) Functional consequences of the human DMT1 mutation on protein expression and iron uptake, *Blood 106*, 3985−3987.
20. Lam-Yuk-Tseung, S., Mathieu, M., and Gros, P. (2005) Functional characterization of the E399D DMT1/NRAMP2/SLC11A2 protein produced by an exon 12 mutation in a patient with microcytic anemia and iron overload, *Blood Cells, Mol. Dis. 35*, 212−216.
21. Lee, P. L., Gelbart, T., West, C., Halloran, C., and Beutler, E. (1998) The human Nramp2 gene: characterization of the gene structure, alternative splicing, promoter region and polymorphisms, *Blood Cells, Mol. Dis. 24*, 199−215.
22. Canonne-Hergaux, F., Gruenheid, S., Ponka, P., and Gros, P. (1999) Cellular and subcellular localization of the Nramp2 iron transporter in the intestinal brush border and regulation by dietary iron, *Blood 93*, 4406−4417.
23. Tabuchi, M., Tanaka, N., Nishida-Kitayama, J., Ohno, H., and Kishi, F. (2002) Alternative splicing regulates the subcellular localization of divalent metal transporter 1 isoforms, *Mol. Biol. Cell 13*, 4371−4387.
24. Johnson, D. M., Yamaji, S., Tennant, J., Srai, S. K., and Sharp, P. A. (2005) Regulation of divalent metal transporter expression in human intestinal epithelial cells following exposure to nonhaem iron, *FEBS Lett. 579*, 1923−1929.
25. Hubert, N., and Hentze, M. W. (2002) Previously uncharacterized isoforms of divalent metal transporter (DMT)-1: implications for regulation and cellular function, *Proc. Natl. Acad. Sci. U.S.A. 99*, 12345−12350.
26. Gruenheid, S., Canonne-Hergaux, F., Gauthier, S., Hackam, D. J., Grinstein, S., and Gros, P. (1999) The iron transport protein NRAMP2 is an integral membrane glycoprotein that colocalizes with transferrin in recycling endosomes, *J. Exp. Med. 189*, 831−841.
27. Touret, N., Furuya, W., Forbes, J., Gros, P., and Grinstein, S. (2003) Dynamic traffic through the recycling compartment couples the metal transporter Nramp2 (DMT1) with the transferrin receptor, *J. Biol. Chem. 278*, 25548−25557.
28. Lam-Yuk-Tseung, S., Touret, N., Grinstein, S., and Gros, P. (2005) Carboxyl-Terminus Determinants of the Iron Transporter DMT1/SLC11A2 Isoform II (-IRE/1B) Mediate Internalization from the Plasma Membrane into Recycling Endosomes, *Biochemistry 44*, 12149−12159.
29. Bonifacino, J. S., and Traub, L. M. (2003) Signals for sorting of transmembrane proteins to endosomes and lysosomes, *Annu. Rev. Biochem. 72*, 395−447.
30. Lam-Yuk-Tseung, S., Govoni, G., Forbes, J., and Gros, P. (2003) Iron transport by Nramp2/DMT1: pH regulation of transport by 2 histidines in transmembrane domain 6, *Blood 101*, 3699−3707.
31. Banerjee, D., Flanagan, P. R., Cluett, J., and Valberg, L. S. (1986) Transferrin receptors in the human gastrointestinal tract. Relationship to body iron stores, *Gastroenterology 91*, 861−869.
32. Anderson, G. J., Powell, L. W., and Halliday, J. W. (1990) Transferrin receptor distribution and regulation in the rat small intestine. Effect of iron stores and erythropoiesis, *Gastroenterology 98*, 576−585.
33. Yeh, J. I., Verhey, K. J., and Birnbaum, M. J. (1995) Kinetic Analysis of Glucose Transporter Trafficking in Fibroblasts and Adipocytes, *Biochemistry 34*, 15523−15531.
34. Petris, M. J., Camakaris, J., Greenough, M., LaFontaine, S., and Mercer, J. F. (1998) A *C*-terminal di-leucine is required for localization of the Menkes protein in the trans-Golgi network, *Hum. Mol. Genet. 7*, 2063−2071.
35. Petris, M. J., and Mercer, J. F. (1999) The Menkes protein (ATP7A.; MNK) cycles via the plasma membrane both in basal and elevated extracellular copper using a *C*-terminal di-leucine endocytic signal, *Hum. Mol. Genet. 8*, 2107−2115.
36. Francis, M. J., Jones, E. E., Levy, E. R., Martin, R. L., Ponnambalam, S., and Monaco, A. P. (1999) Identification of a di-leucine motif within the *C*-terminus domain of the Menkes disease protein that mediates endocytosis from the plasma membrane, *J. Cell Sci. 112* (Part 11), 1721−1732.

BI052307M